Journal of Science and Technology – Engineering and Technology for Sustainable Development
Volume 36, Issue 1, March 2026, 017-023

Effect of $SrTi_{0.875}Nb_{0.1}O_3$ Doping on Energy Storage Density of Lead-fFee $Bi_{0.5}Na_{0.5}TiO_3$-$BaTiO_3$ Based Piezoelectric Ceramics

Tran Vu Diem Ngoc*, Nguyen Thi Thao, Dinh Thi Hinh, Tran Van Cuong
Ha Noi University of Science and Technology Ha Noi, Vietnam
Corresponding author: ngoc.tranvudiem@hust.edu.vn

Abstract

Lead-free piezoelectric ceramic of $(0.94\text{-}x)[(Bi_{0.5}Na_{0.5})TiO_3] + 0.06BaTiO_3 + xSrTi_{0.875}Nb_{0.1}O_3$ (abbreviated as BNBT-xSTN) with x equal 0.0, 0.1, 0.2, 0.3, and 0.4 were synthesized using solid state reaction. The mixing of raw materials was ball milled in alcohol for 24 hours and then calcined at 850 °C for 2 hours to form BNBT-xSTN powder. The BNBT-xSTN powders were further shaped and sintered at 1175 °C with a heating rate of 5 °C per minute and held at the sintering temperature for 2 hours. The crystal structure, microstructure, dielectric, ferroelectric, strain, and energy storage density of the BNBT-xSTN ceramics were systematically investigated. The BNBT-xSTN ceramic materials were analyzed using X-ray diffraction (XRD), all samples show a typical perovskite structure without any trace of secondary phase with a crystal structure coexisting in rhombohedral and tetragonal phases (R&T). Scanning electron microscopy (SEM) images showed the grain boundaries and porosity. The highest dielectric constant was 2511 at x equal 0.2. On the other hand, polarization and strain of STN doped on BNBT were induced with various electric fields E equal 40 to 60 kV/cm, the electric field-induced strain curves of the analyzed samples show a phase transition from a ferroelectric phase to a relaxor phase when the STN is doped. The x equal 0.1 sample showed the maximum energy storage density of 0.3 J/cm^3 at E equal 60 kV/cm, corresponding to the W_{rec}/E_{max} value of approximately 5×10^{-3} J/(kV.cm^2). The highest energy storage efficiency value was 97.34 % at x equal 0.3 because of non-energy loss density.

Keywords: BNBT, energy storage density, ferroelectric, lead-free, piezoelectric.

1. Introduction

Piezoelectric materials are widely used in the electronics industry, particularly in actuators and sensor[1]. The most commonly used piezoelectric materials are lead zirconate titanate ($Pb(Zr_xTi_{1-x})O_3$, PZT). It is well known that Pb is a very toxic substance as it can cause damage to humans. Therefore, there is a great need to develop Pb–free piezoelectric ceramics that are environmentally friendly and possess excellent electrical properties for the replacement of existing Pb–based materials [1, 2]. Among a few Pb-free materials available, solid solutions based on $Bi_{0.5}Na_{0.5}TiO_3$ (BNT) such as $Bi_{0.5}Na_{0.5}TiO_3$ - $Bi_{0.5}K_{0.5}TiO_3$ [3], $Bi_{0.5}Na_{0.5}TiO_3$ - $SrTiO_3$ [4] and $Bi_{0.5}Na_{0.5}TiO_3$-$BaTiO_3$ [5-7]. Lead-free piezoelectric ceramic materials, $(1\text{-}x)Bi_{0.5}Na_{0.5}TiO_3$-$xBaTiO_3$ solid solutions showed a high electric field induced strain (EFIS) and high Curie temperature at the rhombohedral-tetragonal morphotropic phase boundary (MPB) when x = 0.06–0.007. The enhancement of EFIS properties of (1-x)BNT-xBT ceramics was explored by doping the impurities in *A/B*-site or ABO_3 compounds.

Furthermore, many researchers have investigated $Bi_{0.5}Na_{0.5}TiO_3$-$BaTiO_3$ (abbreviated as BNBT) ceramics with an amount of 6 mol% BT showed a high piezoelectric constant of 122 pC/N and a dielectric constant of 3000 [5]. The BNBT ceramics play an important role in reducing the applied field and achieving a large strain, the material can be used for practical applications [2-6]. Besides, BNBT-based was modified by $SrTi_{0.875}Nb_{0.1}O_3$ to exhibit high dielectric constants and low remnant polarization, which delivers much higher energy storage [7]. However, this was applied in higher electric fields ($E \geq 80$ kV/cm).

Besides batteries and supercapacitors, dielectric capacitors are considered a promising device for electrical energy storage [8-12]. The dielectric capacitor has ultrahigh power density with fast charge/discharge rates and no chemical reaction occurring during the charge/discharge processes. A high energy storage of dielectric materials means more energy can be stored in a certain volume, which favors miniaturization, lightweight, and low cost when used in consumer electronics and pulsed power systems [8-12]. However, the required electric field (up to 8 kV/mm) for a phase transition to achieve a large strain, while that of PZT required 3–4 kV/mm and may limit their use in practical applications. In this study, the $(0.94\text{-}x)$ $[(Bi_{0.5}Na_{0.5})TiO_3] + 0.06BaTiO_3 + xSrTi_{0.875}Nb_{0.1}O_3$ (BNBT-xSTN) with x equal 0.0, 0.1, 0.2, 0.3, and 0.4 were synthesized using solid-state reaction with low electric field from 40 to 60 kV/cm. It has been carried out to decrease the required external poling field.

p-ISSN 3093-3242
e-ISSN 3093-3579
https://doi.org/10.51316/jst.188.etsd.2026.36.1.3
Received: Apr 15, 2025; Revised: May 19, 2025
Accepted: Jun 6, 2025; Online: Feb 5, 2026.

2. Experimental Procedure

The $(0.94\text{-}x)[(Bi_{0.5}Na_{0.5})TiO_3]+0.06BaTiO_3+ xSrTi_{0.875}Nb_{0.1}O_3$ bulk ceramic was synthesized using a solid-state reaction method. The raw materials are oxide or carbonate of metals: Bi_2O_3 (99%, from China), Na_2CO_3 (99%, from Germany), $BaCO_3$ (99%, China) SrO (99%, from China), TiO_2 (99%, from China), Nb_2O_5 (99,9%, from China) to synthesis the ceramic with x equal 0, 0.1, 0.2, 0.3, 0.4. The experimental procedure is shown in Fig 1.

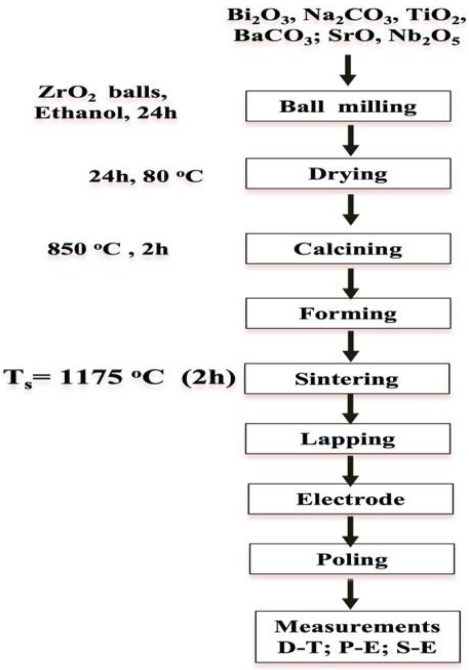

Fig. 1 Experimental procedure of BNBT-xSTN bulk ceramic

The raw materials were weighed according to the proper ratios, and the powder mixture was ground and mixed using alumina grinding balls and an alcohol solvent with a drum mill. The ball-to-powder ratio was 10:1, with a speed of 200 rounds per minute for 24 hours. The slurries were dried to form homogeneous mixing powders. The powder mixtures were calcined at 850 °C for 2 hours to form the BNBT-xSTN material phase. The powders were mixed with a 5% concentration of PVA (Polyvinyl Alcohol – chemical formula $[CH_2CH(OH)]_n$). The amount of PVA added was 0.5g, corresponding to 10% of the weight of each sample. The powder was shaped into pellets with a pressing force of approximately 100–104 MPa. Finally, the compacted pellets were sintered at 1175 °C for 2 hours. The sintered BNBT-xSTN samples were analyzed by Scanning Electron Microscopy (SEM), and its crystal structure was investigated using X-ray Diffraction (XRD). Before measuring the ferroelectric properties, the samples were coated with silver electrodes (using silver paste with 99% purity) on both sides by applying the paste evenly. After applying the silver paste, the samples were fired at 700 °C for 30 minutes. The samples which were analyzed for dielectric constant (ε_r) at temperatures ranging from 30 to 450 °C, were determined using the HP4192A impedance analyzer from the USA. The dielectric constant and dielectric loss at room temperature were analyzed by Hewlett-Packard 4194A. The ferroelectric hysteresis loop of the material (P–E) was observed using the Sawyer-Tower circuit method.

Energy storage density of the BNBT-xSTN was determined by P–E hysteresis loop, it can be rewritten as follows [9-12]:

$$W_{stored} = \int_0^{Pmax} EdP \quad (1)$$

where P_{max} is the polarization at the maximum electric field. Equation 1 was used to estimate the performance of energy storage corresponding to the total area of green and red in Fig. 2.

The energy storage density highly depends upon the permittivity or applied electric field. Because of energy dissipation represented by joule heat loss in dielectric materials, the recoverable energy storage density (W_{rec}) is calculated as:

$$W_{rec} = \int_{P_r}^{Pmax} EdP \quad (2)$$

where P_r is the remnant polarization. The stored energy would be partially dissipated in the form of heat caused by dielectric loss and electrical conduction. Energy efficiency (η) is a reasonably critical parameter for dielectric capacitors, given by:

$$\eta = \frac{W_{rec}}{W} = \frac{W_{rec}}{W_{rec} + W_{loss}} \quad (3)$$

where W_{loss} is the energy loss density, equal to the red shaded area in Fig. 2, [4, 8].

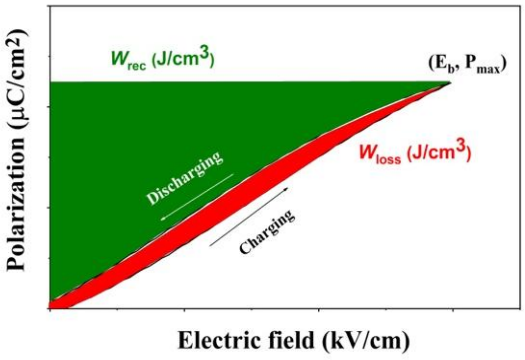

Fig. 2. Illustration of evaluating energy storage performance of a dielectric capacitor has established on the unipolar P-E loop

3. Results and Discussion

The BNBT-*x*STN samples were analyzed for their crystal structure using X-ray diffraction analysis (Fig. 3). The diffraction results show that all ceramic samples with *x* equal 0.0–0.4 exhibit sharp diffraction peaks of the typical perovskite structure without any trace of secondary phase (according to JCPDS 96-210-3298), indicating that STN has completely diffused into the perovskite structure of BNBT-*x*STN to form a fully homogeneous solid solution.

To further clarify the effect of the STN addition on the phase structure of BNBT ceramics, fine scanning XRD patterns were recorded in the 2θ angle range from 45° to 48° (Fig. 3 (b)). Undoped BNBT ceramics correspond to a mixture of tetragonal and rhombohedral symmetry (MPB) because splitting at both 40° and 46° peaks occurs, which could be attributed to the (111)/ (1$\bar{1}$1) planes of a rhombohedral phase and (002)/ (200) peaks of a tetragonal phase, respectively. This is similar to other studies on BNBT-*x*STN [3, 4] with the (002)/(200) peak splitting as a sign of tetragonal symmetry. It is obvious that the locations of the (002)/(200) diffraction peaks have shifted slightly to the left and had a higher intensity when the *x* concentration increased. This is caused by the difference between the radius of dopant STN and base ceramic BNBT. The ionic radius of Sr^{2+} (R_{Sr2+}=1.32A˚) is smaller than that of the A-site (R_{A2+} = 1.39A˚), while Nb^{5+} (R_{Nb5+}=0.64A˚) has bigger ionic radius compared to Ti^{4+} R_{Ti4+}=0.60A˚) in the B site.

The effect of the STN modifier content on the lattice parameters, a and c, estimated from the (002)/(200) peaks is shown in Fig. 4. Careful observation of {200} reflections at form 45° to 48° (Fig. 3b) indicates that STN content increases the gap between (002) and (200) reflections, the lattice constant *a* and *c* increase when doping level lower than 0.4, however the *c* value increased significantly when STN was 0.4.

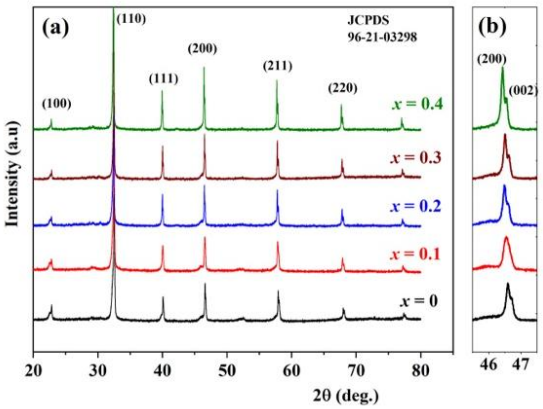

Fig. 3. X-ray diffraction patterns of BNBT-xSTN ceramics (*x* = 0–0.4) between the angle of (a) 20–80 degrees, (b) 45–48 degrees

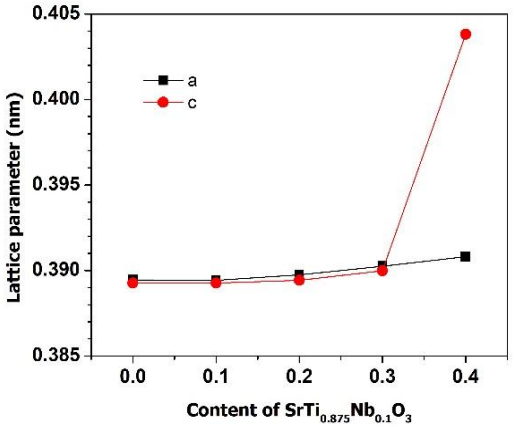

Fig. 4. Lattice parameters *a* and *c* of BNBT-xSTN samples

Fig. 5 displays the SEM analysis of thermally etched BNBT-*x*STN samples with *x* values ranging from 0.0 to 0.4. The examination reveals that the samples possess a high density and well-developed grains. For undoped STN, the microstructure exhibited small grains and a porous structure. The grain size increased when *x* equal 0.4. No grain-boundary phases were observed, suggesting that variations in STN content did not significantly affect grain growth among the different compositions.

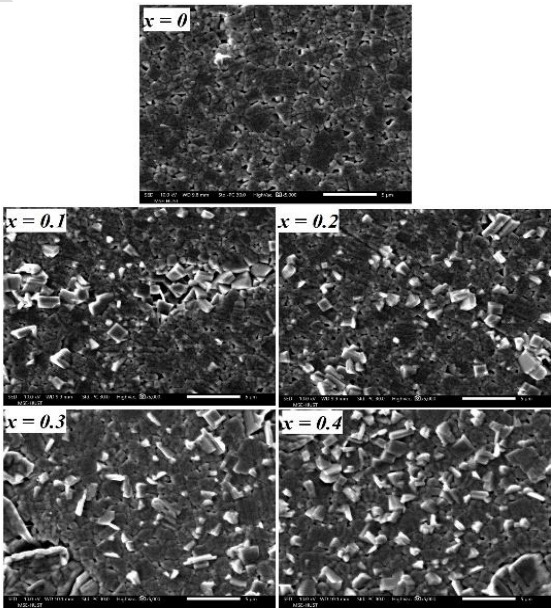

Fig. 5. SEM microstructure of the BNBT-xSTN ceramics with *x* equal 0–0.4

The dielectric constant ε_r of the ceramic material was determined at various temperatures ranging from 25 to 450 °C. Poled BNBT-*x*STN ceramics displayed two abnormal peaks [4-7]. The first peak, located in the lower temperature region, corresponds to T_{F-R} (the ferroelectric–to–relaxor transition temperature), while the second peak is referred to as T_m, denoting the

temperature that yields the maximum dielectric constant. Temperature-dependent dielectric spectra indicated that $T_{F–R}$ decreased below room temperature with increasing STN concentration, revealing a transformation of the phase structure from ferroelectric to ergodic relaxor [7]. The results show that when x is equal to 0, the dielectric constant rises with increasing temperature, reaching a maximum value of 4100 at 280 °C (T_m), after which it declines as the ceramic material transitions to paraelectric. As x increases, the maximum dielectric constant gradually diminishes, and T_m shifts toward room temperature. At x greater than 0.2, the dielectric constant decreases as a function of temperature [7].

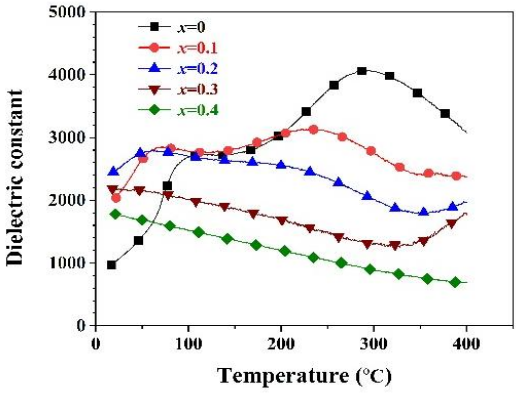

Fig. 6. Dielectric constant as a function of temperature of BNBT-xSTN (x = 0–0.4) ceramics

Dielectric constant and loss at room temperature were determined as shown in Table 1, the highest dielectric constant is 2511 at x equal 0.2. This indicates that higher x values enhance the dielectric properties of the material, improving both the dielectric constant and reducing the tangent loss, thus suggesting better overall performance. The dielectric material required a loss tangent value less than 0.1, which has lower electrical energy dissipation. In this study, the dielectric loss of all samples was lower than 0.04, these results satisfied with dielectric materials for electrical energy dissipation.

Table 1. Dielectric constant at room temperature of BNBT-xSTN (x = 0–0.4)

x	Dielectric constant	Dielectric loss
0	1066	0.05
0.1	2095	0.04
0.2	2511	0.03
0.3	2180	0.03
0.4	1768	0.03

Electric field-induced strain (S-E) with different E values is presented as shown in Fig. 7, the strain value of the samples was increased as a function of the electric fields. Undoped STN (x = 0), the S-E curve was shown as butterfly-shaped with negative strain, which was ferroelectric material when applying electric fields of 40–60 kV/cm. However, when STN was doped on BNBT, the negative strain disappeared (S_{neg} = 0), because of phase transition from ferroelectric to relaxor ferroelectric. The highest strain value was obtained with 0.1 STN doped, at which point co-existence of ferroelectric and relaxor ferroelectric phases was observed. The BNBT-xSTN ceramics ferroelectric properties were evaluated using the Sawyer-Tower circuit at 5 Hz at room temperature with various electric fields from 40 to 60 kV/cm as shown in Fig. 8. Similar with other reports [4-7], the undoped specimen (BNBT) shows saturated square-shaped P–E loops that a distinct ferroelectric behavior regarding both high remnant polarization (P_r) and coercive field (E_c). When BNBT was doped STN, the P-E loops became thinner with P_r and E_c equal 0, proving that the material system has the properties of relaxor ferroelectric.

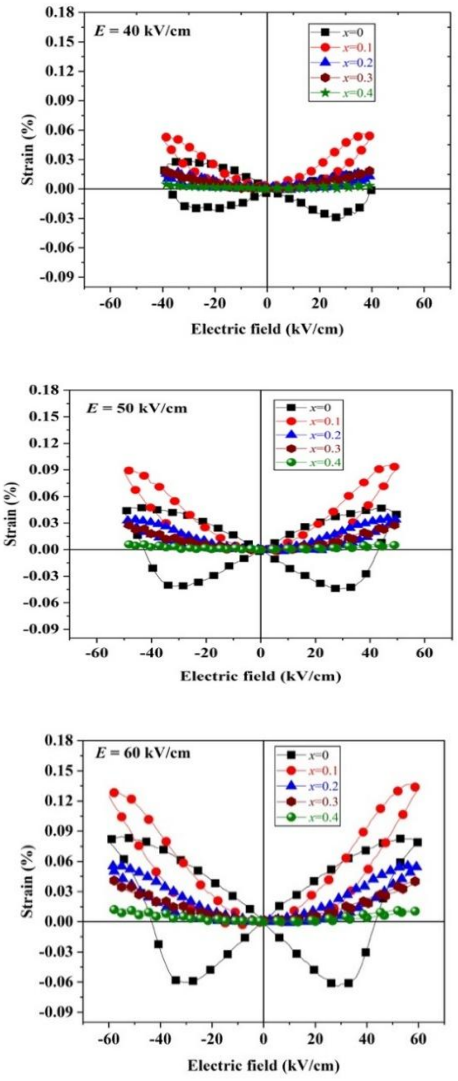

Fig. 7. Electric field-induced strain (S-E) of BNBT-xSTN ceramics at different electric fields

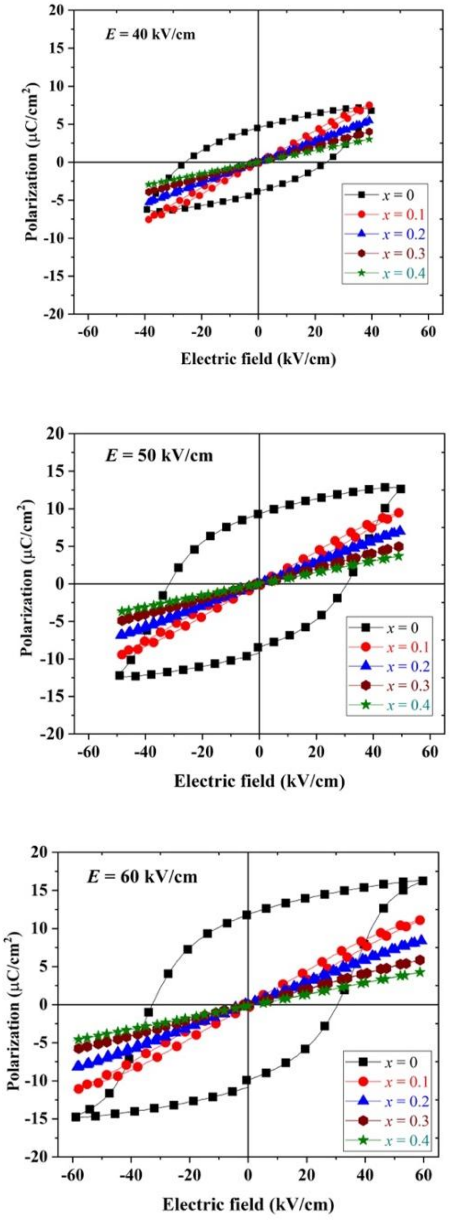

Fig. 8. Polarization hysteresis loop (*P-E*) of BNBT-xSTN ceramics at different electric fields

The maximum (P_{max}) and remnant polarization values of BNBT-*x*STN ceramic at various electric fields are shown in Table 2, the P_{max} and P_r decrease with a high content of STN.

On the other hand, the energy storage density (W_{rec}) and efficiency (η) can be determined from (2) and (3). The corresponding P_{max}, P_r value from Fig. 8, and the P_{max}-P_r values of all samples are calculated in Table 2. The energy storage capacities of all BNBT-STN at 40 kV/cm were shown in Fig. 9. The W_{rec} and W_{loss} are displayed by the green and red area, respectively. The green area of undoped BNBT is smaller than that of BNBT-STN. Conversely, the red area of undoped BNBT is larger than BNBT-STN.

Table 2. Maximum and remnant polarization of BNBT-STN ceramic at various electric field

E	*x*	P_{max}	P_r	P_{max} - P_r
40kV/cm	0	7.2	4.6	3.6
	0.1	7.5	0.1	7.4
	0.2	5.5	0	5.5
	0.3	4	0	4
	0.4	3	0	3

E	*x*	P_{max}	P_r	P_{max} - P_r
50kV/cm	0	12	9.4	2.6
	0.1	9.5	0.3	9.2
	0.2	7	0	7
	0.3	5	0	5
	0.4	3.7	0	3.7

E	*X*	P_{max}	P_r	P_{max} - P_r
60kV/cm	0	16.4	11.8	4.6
	0.1	11.12	0.5	10.62
	0.2	8.4	0	8.4
	0.3	5.8	0	5.8
	0.4	4.6	0	4.6

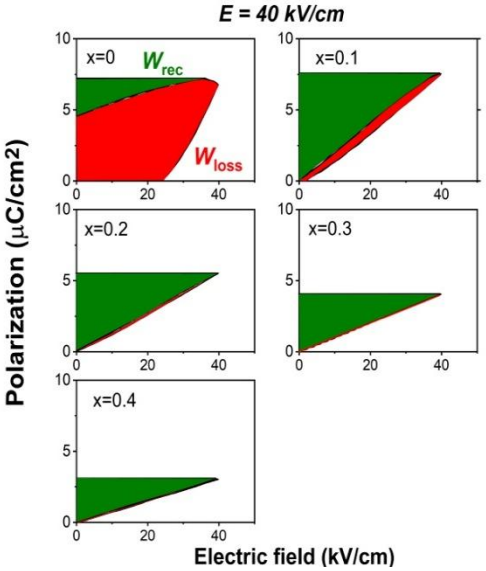

Fig. 9. The energy storage capacities of BNBT-STN samples as a function of *x* under an applied electric field of 40 kV/cm

The energy properties of the dielectric ceramic samples are calculated from the *P-E* loop data using (1)–(3), [7-12]. The recoverable energy storage density (W_{rec}), loss energy, and energy efficiency (η) of BNBT-STN at 40 kV/cm were shown in Fig. 10, the W_{rec} was increased to 0.14 J/cm^3 at *x* equal 0.1 and then decreased at higher STN content, the W_{loss} was reduced when increasing STN content white the η was increased to achieve 95.6 %. Improvement of η value can be

explained by relaxor ferroelectric performance in BNBT-STN samples.

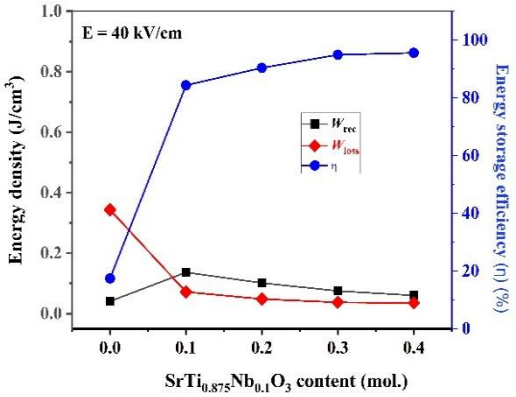

Fig. 10. W_{rec}, W_{loss} and η of BNBT-STN samples as a function of x under an applied electric field of 40 kV/cm

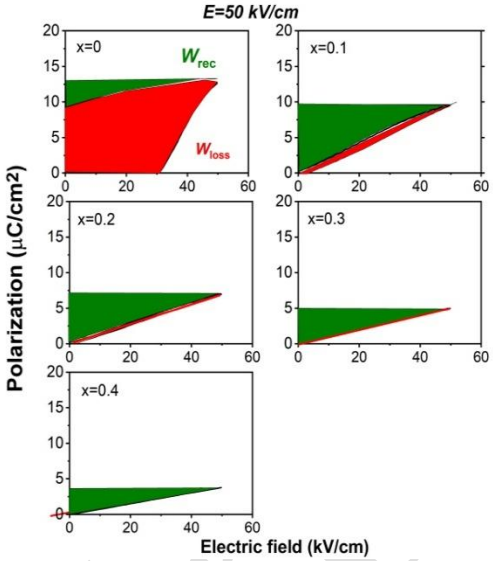

Fig. 11. The energy storage capacities of BNBT-STN samples as a function of x under an applied electric field of 50 kV/cm

When the electric field increased to 50 kV/cm, the energy storage capacities of all BNBT-STN were shown in Fig. 11. The green and red areas of those samples exceeded 40 kV/cm. The recoverable energy storage density (W_{rec}), loss energy, and energy efficiency of BNBT-STN at 50 kV/cm were shown in Fig. 12, the W_{rec} was increased to 0.22 J/cm^3 at x equal 0.1 and then decreased. At the same time, at higher STN content, the W_{loss} was reduced when increasing STN content, white the energy storage efficiency η was increased to achieve 95.6 %.

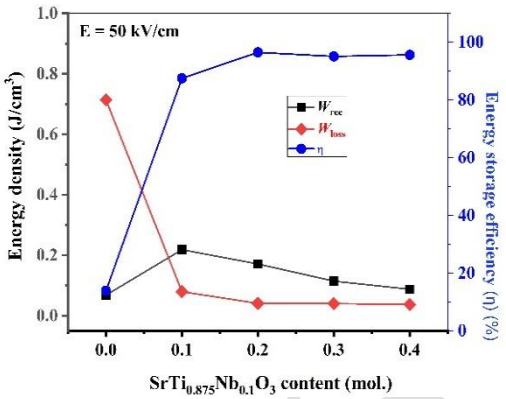

Fig. 12. W_{rec}, W_{loss} and η of BNBT-STN samples as a function of x under an applied electric field of 50 kV/cm

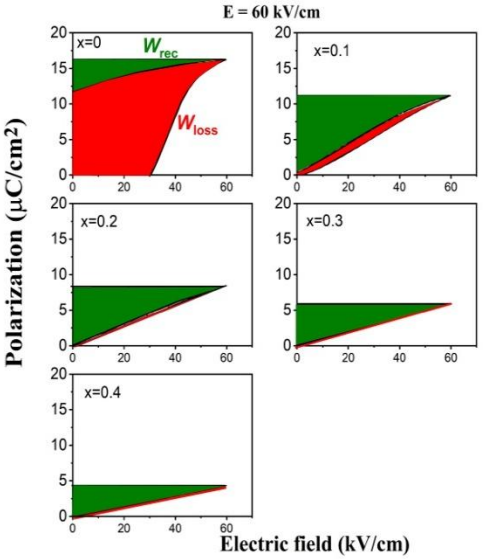

Fig. 13. The energy storage capacities of BNBT-STN samples as a function of x under an applied electric field of 60 kV/cm

The energy storage capacities of BNBT-STN samples at 60 kV/cm were shown in Fig. 13. The green and red areas of those samples were larger because both of maximum polarization and the electric field are increased. The recoverable energy storage density (W_{rec}), loss energy, and energy efficiency of BNBT-STN at 60 kV/cm were shown in Fig. 14. The W_{rec} was increased to 0.3 J/cm^3 at x equal 0.1 and then decreased at higher STN content. While W_{loss} was reduced, corresponding to an increase η to achieve 97.34 %. The highest W_{rec} was 0.3 J/cm^3 at E equal 60 kV/cm, while the energy storage efficiency corresponding to W_{rec}/E_{max} value of 5×10^{-3}[J/(kV.cm^2)] and energy storage efficiency of 87%.

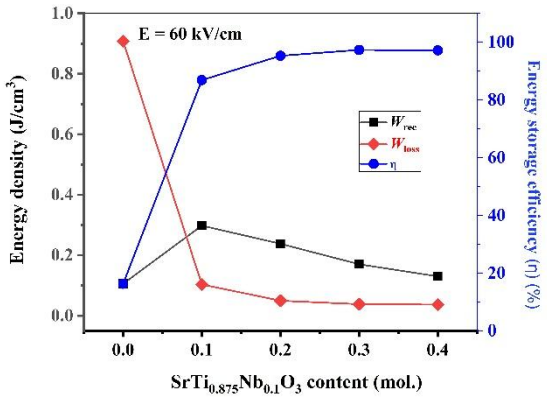

Fig. 14. W_{rec}, W_{loss} and η of BNBT-STN samples as a function of x under an applied electric field of 60 kV/c

6. Conclusion

The effect of $SrTi_{0.875}Nb_{0.1}O_3$ doping on energy storage density of lead-free $Bi_{0.5}Na_{0.5}TiO_3$-$BaTiO_3$ based piezoelectric ceramics has been successfully synthesized by using solid-state reaction. The material has a single perovskite structure with a morphology phase boundary coexisting in rhombohedral and tetragonal phases. The BNBT samples were changed from ferroelectric to relaxor ferroelectric by STN doped, the relaxor ferroelectric phase exhibits a low W_{loss} and high energy efficiency. The highest dielectric constant at room temperature was 2511 at x equal 0.2. The x equal 0.1 sample showed the maximum energy storage density of 0.3 J/cm^3 at E equal 60 kV/cm, corresponding to the W_{rec}/E_{max} approximate value of 5×10^{-3} J/(kV.cm^2). The highest energy storage efficiency value was 97.34 % at x equal 0.3 because of non-energy loss density. The obtained results are an important promise for researching the application of piezoelectric ceramics to replace lead-based materials in the future.

Acknowledgments

This work was supported by the Hanoi University of Science and Technology under the Grant T2023-PC055.

References

[1] K. Uchino, Ferroelectric Devices, Marcel Decker, Inc., New York, USA, 2000.

[2] J. Wu, Perovskite lead-free piezoelectric ceramics, Journal of Applied Physics, vol. 127, iss. 19, May 2020, Art. no. 190901. https://doi.org/10.1063/5.0006261

[3] V. D. N. Tran, Aman Ullah, T. H. Dinh, and Jae-Shin Lee, Large field-induced strain properties of $Sr(K_{0.25}Nb_{0.75})O_3$-modified $Bi_{1/2}(Na_{0.82}K_{0.18})_{1/2}TiO_3$ lead-free piezoelectric ceramics, Journal of Electronic Materials, vol. 45, iss. 5, pp. 2627–2631, Mar. 2016. https://doi.org/10.1007/s11664-016-4445-1

[4] Thi Hinh Dinh, Vu Diem Ngoc Tran, Nguyen Thi Thao, Vinh Le Van, and Ky Nam Pham, Enhanced energy storage density and efficiency of lead-free $Bi_{0.5}Na_{0.5}TiO_3$-$SrTiO_3$ ferroelectric ceramics by $BaZrO_3$ doping, Journal of Science and Technology: Engineering and Technology for Sustainable Development, vol. 32, no. 1, pp. 009–016, Mar. 2022. https://doi.org/10.51316/jst.156.etsd.2022.32.1.2

[5] B. J. Chu, Da-Ren Chen, G-R. Li, and Q-R Yin, Electrical properties of $Na_{1/2}Bi_{1/2}TiO_3$–$BaTiO_3$ ceramics, Journal of the European Ceramic Society, vol. 22, iss. 13, pp. 2115–2121, Dec. 2002. https://doi.org/10.1016/S0955-2219(02)00027-4

[6] T. H. Dinh, H-S Han, V. D. N. Tran. V. L. Van, N. B. Hung, and J-S Lee, 0.4% Electrostrain at low field in lead-free Bi-based relaxor piezoceramics by La doping, Journal of Electronic Materials, vol. 49, no. 10, pp. 6080–6086, Aug. 2020. https://doi.org/10.1007/s11664-020-08348-8

[7] J. Shi, X. Liu, and W. Tian, High energy-storage properties of $Bi_{0.5}Na_{0.5}TiO_3$-$BaTiO_3$-$SrTi_{0.875}Nb_{0.1}O_3$ lead-free relaxor ferroelectrics, Journal of Materials Science & Technology, vol. 34, pp. 2371–2374, Dec. 2018. https://doi.org/10.1016/j.jmst.2018.06.008

[8] Z. Yang, H. Du, L. Jin, and D. Poelman, High-performance lead-free bulk ceramics for electrical energy storage applications: design strategies and challenges, Journal of Materials Chemistry A, vol. 9, pp. 18026–18085, Jul. 2021. https://doi.org/10.1039/D1TA04504K

[9] G. Wang, Z. Lu, Y. Li, H. Ji, A. Feteira, D. Zhou, D. Wang, and I. M. Reaney, Electroceramics for high-energy density capacitors: current status and future perspectives, Chemical Reviews, vol. 121, iss. 10, pp. 6124–6172, Apr. 2021. https://doi.org/10.1021/acs.chemrev.0c01264

[10] W. Zhu, Z-Y Shen, W. Deng, K. Li, W. Luo, F. Song, X. Zeng, Z. Wang, and Y. Li, A review: $(Bi,Na)TiO_3$ (BNT)-based energy storage ceramics, Journal of Materiomics, vol. 10, iss. 1, pp. 86–123, Jan. 2024. https://doi.org/10.1016/j.jmat.2023.05.002

[11] F. Yan, J. Qian, S. Wang, and J. Zhai, Progress and outlook on lead-free ceramics for energy storage applications, Nano Energy, vol. 123, May 2024, Art. no. 109394. https://doi.org/10.1016/j.nanoen.2024.109394

[12] Thi Hinh Dinh, Vu Diem Ngoc Tran, Tu Le Manh, and Jae-Shen Lee, Effects of $BaZrO_3$ on the phase evolution and energy storage capacities of BNT-based lead-free dielectric ceramics, Journal of Physics and Chemistry of Solids, vol. 198, Mar. 2025, Art. no. 112462. https://doi.org/10.1016/j.jpcs.2024.112462